UHF Epidermal Sensors: Technology and Applications

S. Amendola[1,2], C.Occhiuzzi[1,2], C. Miozzi[1], S. Nappi[1]
F. Amato[1], F. Camera[1], G.Marrocco[1,2]

[1] *University of Roma Tor Vergata,*
[2] *Radio6ense srl*

November 6, 2019

Abstract

Originally introduced by the material science community, *skin-mounted electronics* is nowadays the new frontier for unobtrusive body-centric monitoring systems. Current advances of the Radiofrequency Identification (RFID) technology can boost this emerging class of bio-integrated devices exploiting low-power (even passive) wireless communication and sensing interfaces. This contribution resumes the performance of UHF RFID epidermal antennas, their optimal size and the upper bounds in the achievable radiation gains. Some promising application scenarios are described by realistic experimentations, concerning the remote and unobtrusive monitoring of relevant health parameters (temperature, breathing, sweat, pH) for healthcare, wellness and sports. Finally, the latest research on the next integration of epidermal transponders within the incoming 5G communication networks is highlighted.

1 Introduction

The next wave beyond *wearable electronics* is represented by *bio-integrated technology*, a novel multidisciplinary research trend that aims at re-shaping the flat and rigid wafer-based electronics around the soft and curvilinear surfaces of living organisms. The epidermis is indeed an exceptionally complex, time-evolving interface that provides a precious insight about people's health and wellbeing. Its essential functions include physical protection against environmental agents, temperature regulation and water retention. The skin undergoes significant physiological changes earlier than central organs, which are protected by homeostatic feedback. It is also the primary perceptual interface towards the surrounding environment and it is continuously "sampled" by the central nervous system in terms of tactile cues. At a social and psychological level, skin even plays a role in establishing interpersonal bonds. Basically, the skin constantly
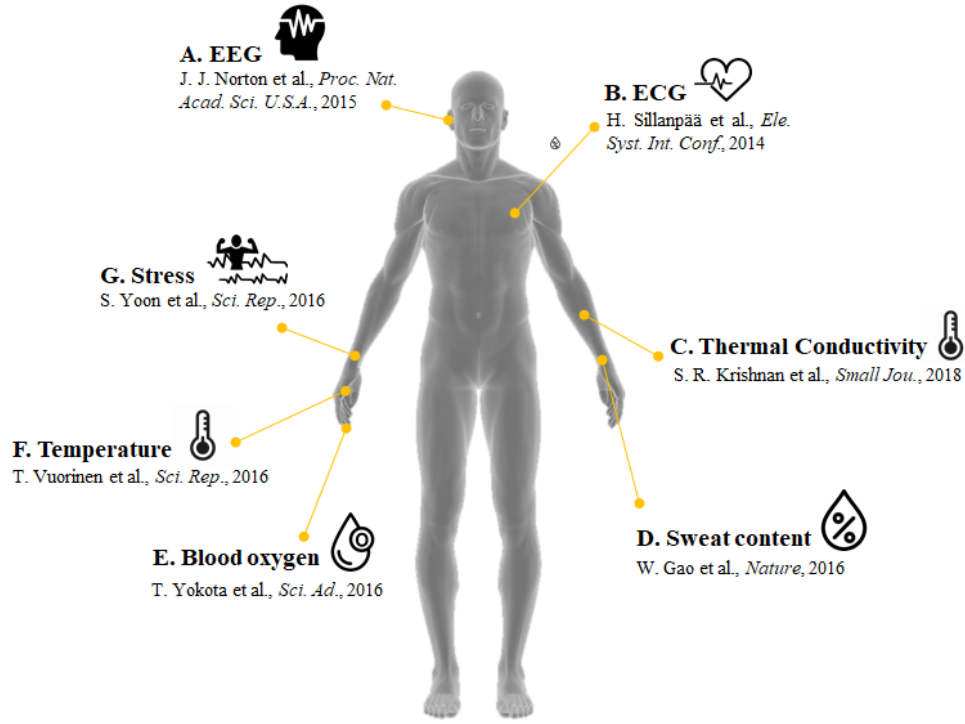
1

Figure 1: State-of-the-art Epidermal devices Systems for measuring: (A) Electroencephalogram, (B) electrocardiogram, (C) thermal conductivity, (D) sweat content, (E) blood oxygen, (F) temperature, (G) stress.

conveys two-directional data flow, from the internal body to the external environment and vice-versa. In line with this twofold role, skin-mounted devices are envisaged to have the double functionalities of *i)* non-invasively collecting biophysical parameters over the epidermis and *ii)* acting as invisible probes able to replace damaged sensory functions and even to extend the human perception and sensing capabilities (e.g. tactile, thermal) beyond the their limits.

Being pioneered in the last decade by Material scientists, the *Epidermal/Skin Electronics* [1] has witnessed an unprecedented worldwide prolific scientific activity that resulted in developing ultrathin, flexible, stretchable and even transient tattoo-like electronics systems whose physical properties (thickness, thermal mass and elasticity) resemble those of the skin. Accordingly, these bio-integrated devices are suitable to tightly adhere to the epidermis. They can sample physiological indicators (temperature [3, 4], pH [5], bio-potentials [6, 7], blood oxygen [8], hydration [9]) and eventually act as controlled actuators able to trigger therapeutic actions (e.g. the transdermal drugs release, neuro-stimulator, local heating) [2].

More recently, research efforts were dedicated to the design of ad-hoc skin antennas and communication modules to provide this new class of skin-sensors with the capability of wirelessly transmit (even in battery-less mode) the relevant data measured over the body toward remote hubs where signals are stored and processed for generating reports and even alarms in case of anomalies.

In this scenario, the passive UHF[1] Radiofrequency Identification (RFID) technology [10], which is widely adopted in logistics, is now mature enough to foster the concrete usability of skin-devices in real applications. The communication through electromagnetic backscattering, as in the RFID architecture, requires just a small battery-less IC transponder that is inherently suited to the integration within flexible, lightweight and ultrathin membranes, and offers jointed communication and sensing capabilities without the need of adding complex circuitry.

This chapter reviews the latest advances in Epidermal Electromagnetics, focusing on the investigation of electromagnetic performance of UHF radiators interfacing with human body with high loss and high permittivty, the natural bounds, the achievable reading ranges and the technological research on bio-materials and manufacturing technologies for fabrication of epidermal transponders. Examples of RFID epidermal sensors tested in real-life scenarios are then described, concerning the monitoring of body temperature, breathing and training activities of athletes and workers exposed to harsh environments. Finally, future trends and open challenging regarding the integration of skin devices within the incoming 5G framework are discussed.

2   Rationale of UHF epidermal antennas

The early prototypes of skin-tight sensors described in literature - despite their tattoo-like conformability and stretchability - relayed on bulky batteries and tangled wires for power supply and data transfer, that hindered the wearers' comfort and natural movements. First attempts to establish wireless powering and communication considered the HF/NFC near-field reading at 13.56 MHz based on the inductive coupling of resonant LC circuits to external reading coils [11, 12, 13, 14]. At the HF band, the limited sensitivity of antennas to the underlying human tissues greatly simplifies the design of the radiators, which basically consist of multi-turns coils. Another undoubted advantage of this approach is the possibility to use an NFC-equipped smartphone for data retrieval. Nevertheless, since the reading device must be positioned very close (typically few centimeters) to the skin[2], the usability of NFC is strongly limited to supervised and cooperative monitoring (self-assisted personal tracking, and user-oriented), with one sensor readable at once. The UHF RFID standard (860 - 960 MHz) is instead particularly attractive over the HF one, due to the potential for improvement of the activation ranges up to one meter (or more)

---

[1]Ultra High Frequency: 866-956 MHz for wolrdwide RFID applications.

[2]The magnetic field that is at the basis of the inductive coupling decays with the cube of distance,

with the simultaneous reading of multiple sensors at a time. This possibility represents a breakthrough for application scenarios, paving the way to the immersive and non-invasive monitoring of masses of non-cooperating users though remote scanners spread into Smart RFID-enabled Spaces [15] (Fig. 2.a).
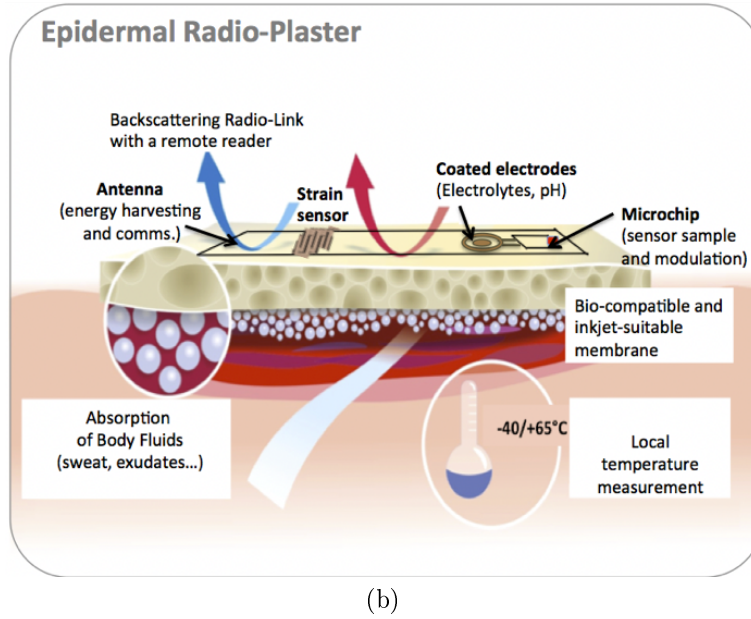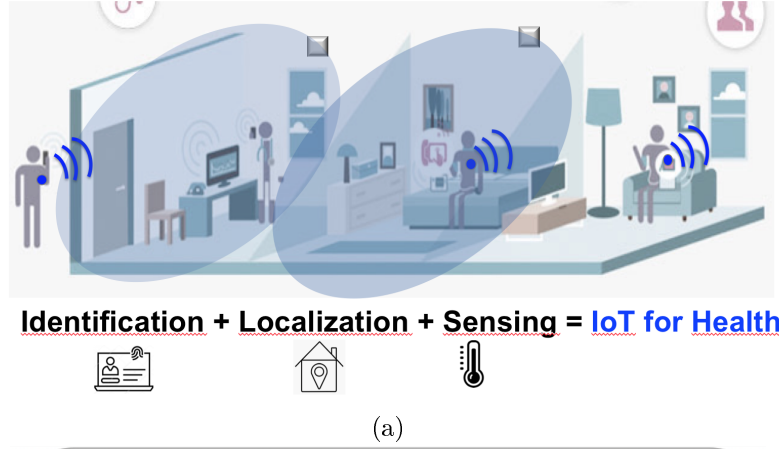

(a)

(b)

Figure 2: (a) Pictorial representation of RFID-enabled spaces for non collaborative monitoring; (b) Concept of the epidermal radio-sensor capable to monitor bioparameters over the skin (temperature, pH, the absorption of skin exudates..) and wirelessly interact with a remote reader

The concept of an epidermal UHF RFID device is sketched in Fig. 2.b.

The transponder comprises a miniaturized antenna for energy harvesting and communication with a remote interrogator, a microchip for data sampling and signal modulation and finally several sensing elements that could be connected to the IC or distributed over the radiator surface (e.g. sensitive coatings). The epidermal tag is deposited on a bio compatible membrane which may dynamically interact with the skin interface by absorbing biofluids (sweat, exudates) or releasing drugs. The resulting epidermal radio-sensor is able to perform a multivariate sensing of local skin features such as temperature, sweat loss and pH, thus realizing a real *Lab on skin*.

The chapter will hereafter focus mostly on UHF systems.

2.1 Communication via backscattering modulation

An UHF RFID system [10] comprises two main elements: i) the remote transponder, or *tag*, including an antenna and a microchip transmitter (IC), located on the object to be identified and ii) the local querying system, or *reader,* that powers up the tag, collects the data backscattered from the tag and eventually performs a preliminary processing. This system conveys various kinds of data, e.g.: a unique identification code (ID), through radio-frequency electromagnetic signals. Most innovative ICs integrate also sensing capabilities by exploiting internal sensors or through an analog interface for external probes.

The tags could be *passive*, harvesting energy from the interrogating system; *semi-active,* when a battery is only used to improve the sensitivity of the IC receiver or to supply embedded sensors; or *fully active,* in case the local power source directly feeds a micro-controller as well as the transmitting radio.

Battery-less tags have an almost unlimited life, low-cost, lightweight and need no maintenance thus providing, in principle, the greatest flexibility for seamless integration of RF devices over the human skin, especially in case of disposable plasters. Nevertheless, a slightly complex circuitry is still accepted if it improves and makes reliable reading or sensing performance in some critical applications. In the latter case, battery-assisted solutions may be exploited as well, thanks to the novel flexible thin-film battery technologies [16, 17] that still permit a certain level of integration into soft skin-attachable patches.

With reference to the RFID architecture sketched in Fig. 2.b, the length of the communication link, i.e. the maximum distance at which a tag can be detected by the reader, is a practical performance indicator of the overall radio system. In case of epidermal antennas, due to the great dissipation of electromagnetic power (with radiation gain generally lower than -10 dBi), shorter reading distances are expected, with intermediate activation ranges between wearable and implantable systems (Fig. 3.b). Moreover, as sensing functionalities provided by the new RFID ICs are achieved at the expense of a reduced power sensitivity ($P_{chip} >$ -10 dBm), the length of the link might be further decreased.

Under simplified hypotesis (free-space interaction, impedance matching, polarization alignment), the reading range for the *direct link* is derived from the

Friis Equation [10] by assuming that the power transmitted from the reader and collected by the tag is equal to the IC sensitivity ($P_{R \to T} = P_{chip}$):

$$d_{forward} = \left(\frac{\lambda_0}{4\pi} \right) \sqrt{\frac{P_{in}G_R G_T}{P_{chip}}} ; \tag{1}$$

and, for the *reverse link*, from the *radar* equation with the power backscattered by the tag towards the interrogator being equal to the reader receiver sensitivity ($P_{T \to R} = P_{reader}$),

$$d_{reverse} = \left(\frac{\lambda_0}{4\pi} \right) \sqrt[4]{\frac{P_{in}G_R^2 G_T^2 \rho}{P_{reader}}} , \tag{2}$$

where P_{chip} is the IC sensitivity, P_{reader} the sensitivity of the reader and ρ the tag backscatter modulation loss. The theoretical maximum reading distance is hence:

$$d_{max} = min \left\{ d_{forward}, \ d_{reverse} \right\}. \tag{3}$$

The RFID link is often forward limited, that is $d_{forward} < d_{reverse}$, when the following condition is satisfied:

$$P_{reader} \leq \rho \frac{P_{chip}^2}{P_{in}} , \tag{4}$$

while the bottleneck is the backward-link if the inequality is reversed.

The nomogram in Fig. 3.b shows the achievable reading range as a function of $\{P_{chip}, P_{reader}\}$ for the reader emitting 3.2 W EIRP, which is the maximum power allowed by the European regulation. The distances reported on the iso-lines are normalized by the square root of the tag's gain which equally impacts on both the direct and return links, so the graph has general validity regardless of the radiator performance.

The read range of pure passive tag with sensing capability is strongly limited by the poor IC sensivity (e.g. $d_{max} \sim 70$ cm for $G_T = -12$ dBi and $P_{chip} = -4$ dBm). By adding a battery the required power to wake up the IC is significantly reduced (down to $P_{chip} = -31$ dBm) with a corresponding increase of d_{max}, which becomes a backward-limited link (e.g. $d_{max} \sim 2$ m for $G_T = -12$ dBi and $P_{chip} = -31$ dBm). The current sensitivity of state-of-the art of the ICs for labeling ($P_{chip} \sim -22dBm$) places passive tags for identification purposes only between the above conditions (see 3.b).
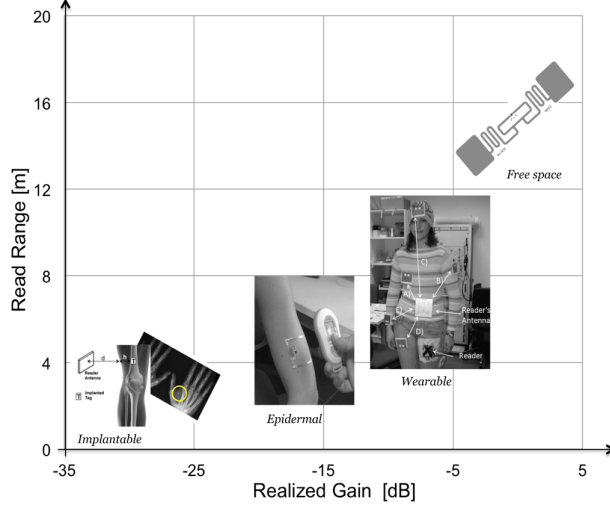
(a)
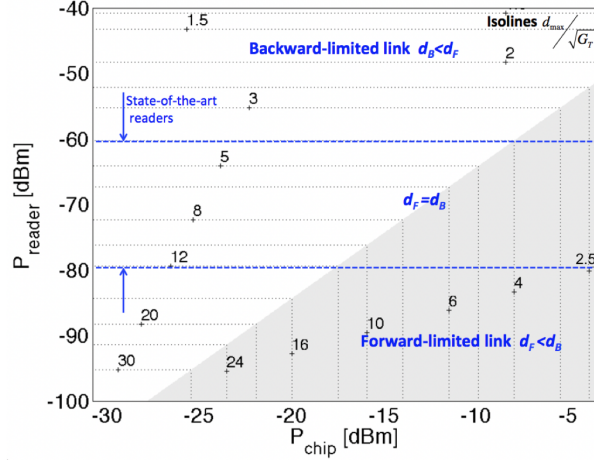
(b)

Figure 3: (a) RFID-Bodycentric Systems: Typical read distances of passive implantable, epidermal, wearable and free-space transponders having a microchip sensitivity of -22 dBm. (b) Graphical representation of eq. 4, in dB-scale, for the identification of the link bottleneck. Isolines of the maximum reading range are normalized by $\sqrt{G_{tag}}$. Without loss of generality, it is assumed that $P_{in}=$ 1 W, $G_R=$ 5 dBi, $\rho=0.04$.

2.2 Upper-bound performance of Epidermal antennas

The colocation of an UHF radiator with the human skin, or with living matter in general, poses an intrinsic challenge due to the high losses of tissues which strongly degrade the radiation efficiency of the antenna and, accordingly, the upper bound communication performance. This problem has been widely addressed in the past by research on wearables antennas: several strategies have been adopted for decoupling the antenna from the lossy body, such as ground planes (patch-like antennas) [18], metamaterials, electromagnetic band gap (EBGs), insulating dielectrics, multilayer spacers placed between the body and dipole, slot, or a loop antenna [19].

However, while wearable antennas are generally integrated within garments and wristbands without any severe constraints of micro-metric thickness, epidermal antennas are conceived to be directly attached over the skin through sub-millimeter thin flexible and/or stretchable membranes. As skin-mounted transponders act, simultaneously, as sensors, transducers and communicating devices, their presence must not interfere with local metabolism of the epidermis to not alter the measurements of bioparameters over the skin surface. Shielding planes, as in the case of patch antennas, have to be avoided and the amount of the metal conductor must be minimized to preserve the natural breathability and heat exchanges at the skin interface.

Before introducing potential implementations of skin RFID antennas, it is hence useful to clarify the role of the geometrical and electrical parameters (shape, size, material of conductors) and the corresponding upper-bound performance achievable for optimal on skin-mounted devices.

For instance, it is well known that the radiating properties of an antenna in free-space are strictly correlated with its physical size (electrically larger antennas have the potential to provide better gain than smaller ones). However, in case of antennas placed on a lossy medium like the human skin, the gain-size relationship is not trivial and not necessarily monotonic. The analysis in [20], considering a set of reference single-layer radiators with different canonical shapes (dipole, loop and their complementary slotted counterparts) over homogenous phantom (30 x 30 x 20 cm^3, $\varepsilon = 49$, $\sigma = 0.9$ S/m,), demonstrates the existence of an optimal size of the skin antennas (from 3 to 6 cm for loops and from 6 to 15 cm for dipoles depending on the attaching membrane) having a fixed upper bounds in the achievable radiation gain (less than -10 dBi in the case of 0.5 mm thick application substrates), that is almost independent on the antenna layout and rather modest because of the high loss of the underlying tissues (numerical results in Table 1). Overall, the loop layout is a good trade-off that permits to considerably minimize both the size and the amount of conductor. The resulting bell-shape relationship between the efficiency/gain and physical size of antennas can be explained by taking into account the presence of two counteracting phenomena, namely the radiation resistance, which is proportional to the overall length of the antenna, and dissipation of power into the conductors and the surrounding tissues, which also increases with the antenna size.

Table 1: Electromagnetic performance and geometrical parameters of the reference epidermal antennas at 870 MHz.

Antenna	η [%]	G [dB]	L_{opt} [cm]	A_{metal} [cm^2]
(vertical bar)	0.3	-18.7	5	0.5
(open circle)	0.3	-19.1	3	0.9
(filled circle with bar)	0.3	-19.4	6	27.6
(filled circle with ring)	0.2	-19.5	8	46.7

The same study also investigates the impact of the quality of the conductors on antenna performance, as many fabrication methods for manufacturing tattoo-like devices often involve sub-optimal conducting materials (silver nanoparticles, biodegradable and even edible paintings). Low-cost inkjet printable paints with conductivity higher than 10^4 S/m could nevertheless provide radiation performance comparable with the copper-made antennas, as the conductivity of the traces has only a second-order impact on the radiation performance which is mainly affected by the tissue losses.

Fig. 4 summarizes some experimental findings obtained through a laboratory setup comprising a transmitting monopole antenna and two different receiving antennas, a monopole and half-square loop attached on a body phantom. The experiment was repeated twice, first time with both tags made of bulk copper, then of silver ink. The two-port measurements corroborated the numerical analysis, by verifying the existence of an optimal size and the upper-bound of the antenna gain when placed over a body-like lossy media. The secondary role of the antenna conductors in the overall performance was also experimentally assessed: as copper and inkjet-printed antennas revealed comparable results, despite the significantly poorer conductivity of the silver nanoparticle ink ($\sigma \sim 10^3$ S/m).
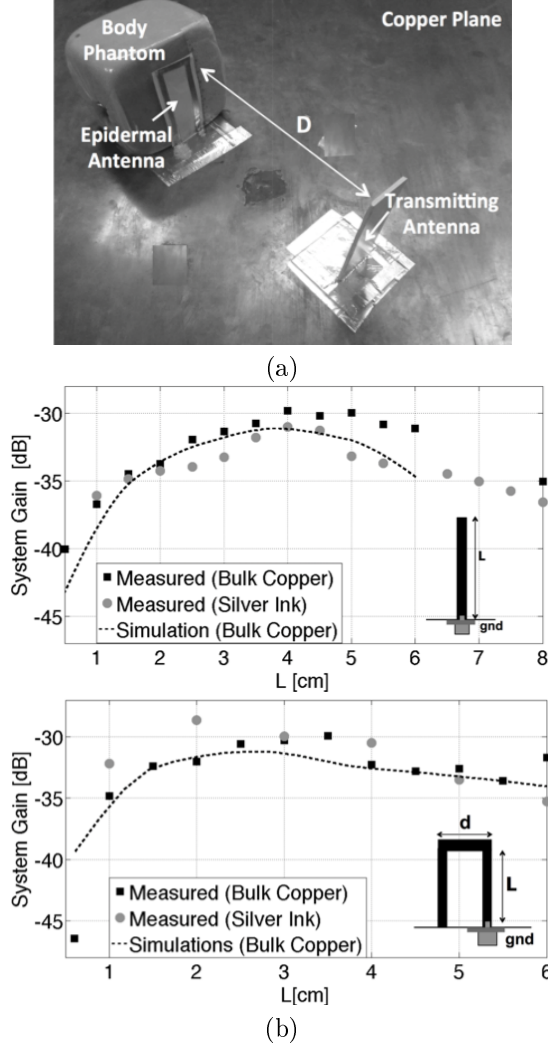
(a)

(b)

Figure 4: (a) Experimental setup for the characterization of epidermal antennas, comprising a reference monopole antenna at distance D = 17 cm from a cooked-pork box (size $10 \times 10 \times 7 \ cm^3$) hosting the monopoles and half-loops under test. The antenna ports were connected to a VNA for measuring the scattering matrix. (b) Measured and simulated system gains g, defined as in [20], at 870 MHz for the prototyped monopoles and half-loops over a cooked-pork phantom versus their vertical size. Antennas were made of adhesive bulk copper and silver nano-ink through inkjet printing on functionalized PET.

3 Examples of UHF epidermal antenna systems and manufacturing

This section presents an overview of the state-of-the-art layouts for UHF epidermal antennas. Manufacturing options and materials are discussed case by case.

3.1 Battery-less epidermal tag

Early examples of UHF skin antennas were in the form of square dual-loops of 5 x 5 cm^2 [21]. The radiators, made of a copper-based flexible adhesive sheet (thickness 35 μm), were carved out by a two-axis digital-controlled cutter and then transferred on the hosting substrate through a transfer tape. Starting from this layout, a smaller version of the tag (2.5 x 5 cm^2) was then implemented by folding the "un-useful" arms having opposite-phase currents and by introducing additional meanderings on the radiating sides providing the radiator with some degree of stretchability [22]. More recently, new-generation ICs with self-tuning capabilities have been integrated within epidermal tags and further miniaturization has been achieved with open loop designs (3 x 3 cm^2) and meandered dipoles shaped to perfectly fit within the area of a fingertip (1.2 x 2 cm^2) for applications as Finger Augmented Devices (FADs) [25, 24].
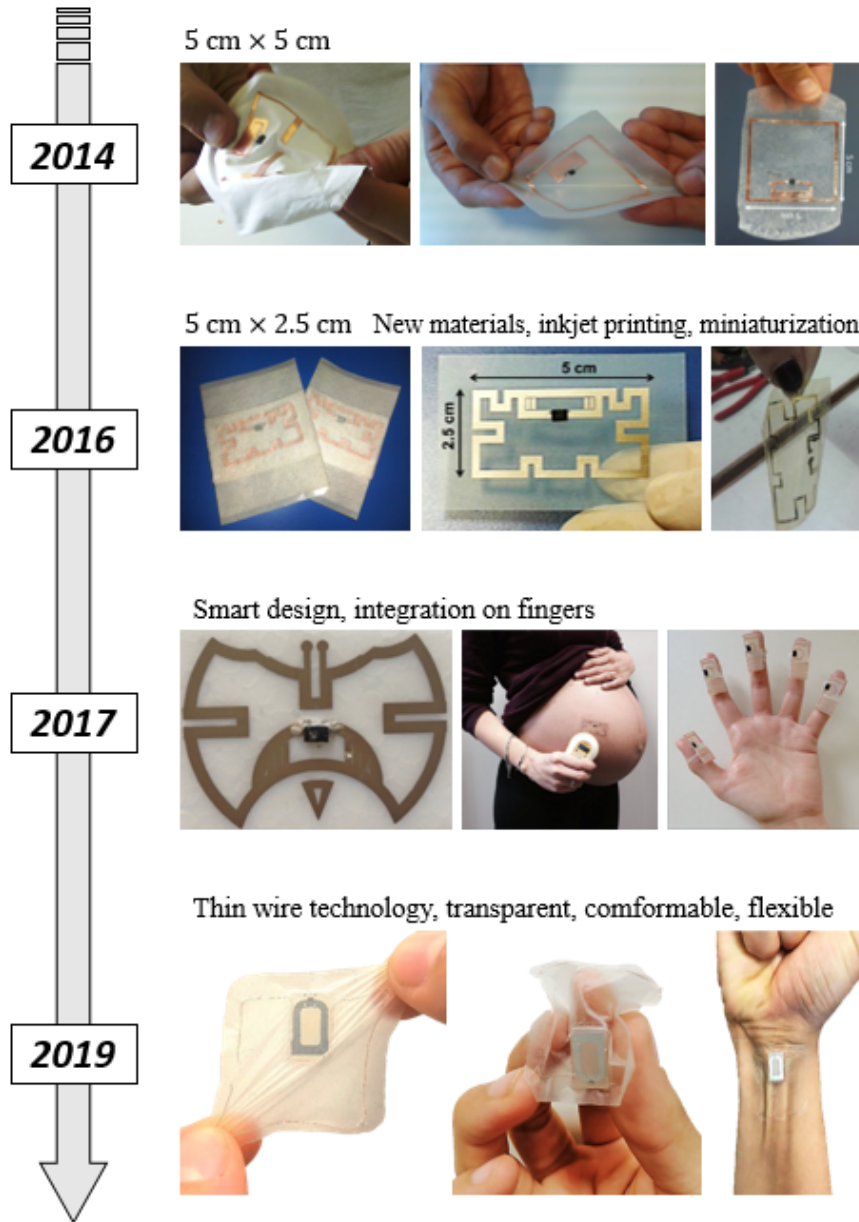
Figure 5: Examples of battery-less UHF RFID epidermal systems.

Several state-of-the-art manufacturing options are suitable for producing skin-mounted transponders: a) digital cutting of flexible adhesive copper, b) deposition of conductive micro-wires, c) low-cost inkjet printing [28] with off-the-shelf printers and self-sintering silver ink [27], and d) gold patterning over

a micrometric Polyimide (PI) through photolithography in a cleanroom. The systematic comparison of the EM performance in [26] revealed that comparable reading distance can be achieved with the described technologies so that the most appropriate manufacturing choice is suggested, case by case, by acceptable costs, processing time, physical robustness, and need of monolithic integration with other sensors. In general, technologies supporting 'additive' approach to production (copper microwire, ink-jet printing) are preferable over 'subtractive' cutting and photolithography processes which, instead, imply waste of conductors with consequence on costs and pollution. Ink-jet printing with off-the-shelf printers is indeed a viable method for the rapid (few seconds) and inexpensive laboratory prototyping of epidermal antennas with sufficient resolution (up to 0.3 mm). Majors limitations concern the selection of printing substrates with *ad-hoc* surface pre-treatment coating: the resistance to cracks and the robustness of interconnections to components (battery, IC sensors). The deposition of electrically conductive wires is an inlay-less and very eco-friendly (no polluting chemicals are used) process which is definitely suitable for low-cost large-scale production with great versatility in terms of shapes, substrate and conductors with different radius and mechanical resistance (aluminum, copper, metalized fibers). The microfabrication remains the benchmark approach for high-resolution layouts, for handling the deposition of ultra-thin (<20 µm) biocompatible substrates and, above all, for the monolithic fabrication of both the radiator and additional flexible electronic components (e.g. piezoelectric sensors) within the same process. This procedure has however very high cost due to the need of cleanroom facilities, photo masks, photolithography chemicals, and manpower that may prevent epidermal sensors from being inexpensive and disposable.

Several flexible membranes were used as substrates for the above epidermal transponders. Being these materials definitely unconventional for RF devices, their dielectric features in the UHF band are mostly unknown, especially in the case of sensitive/functionalized materials whose properties change along with the time according to a target biological process (exposure to biofluids such as sweat and exudates).

The work in [31] describes an efficient low-cost non-destructive method for characterizing the RF properties of skin substrates in both static and dynamic (time-variant) conditions. The setup consists of a multilayered suspended resonator having the ring and the ground plane/feed network in separate planes for the easy placement of samples with different sub-millimetric thickness, shape and size in the middle. The circular slot carved out the suspended structure permits the direct exposition of the membranes to external agents such as liquids, gases and mechanical solicitations. The corresponding RF properties are estimated by an hybrid identification procedure based on 2-port measurements and numerical modeling of the device. Fig. 6 summarizes the properties derived for three main classes of typical skin dressings: *a)* non-reactive polymeric membranes that acts as physical support to the electronics without interacting with the skin interface (e.g. medical-grade biosilicone, fibrous plasters, dressings made of transversely stretchable non-woven polyester like the Fixomull®,

bioresobable synthetic scaffolds made of Poli(ε-caprolactone) (PCL) produced by electrospinning); *b)* films able to reversely absorb and release body fluids at skin interface (hydrogels for applications on wounds care and controlled transdermal drugs release [30]) c) moisture-retentive dressings undergoing through irreversible transformation after exposure to fluids.
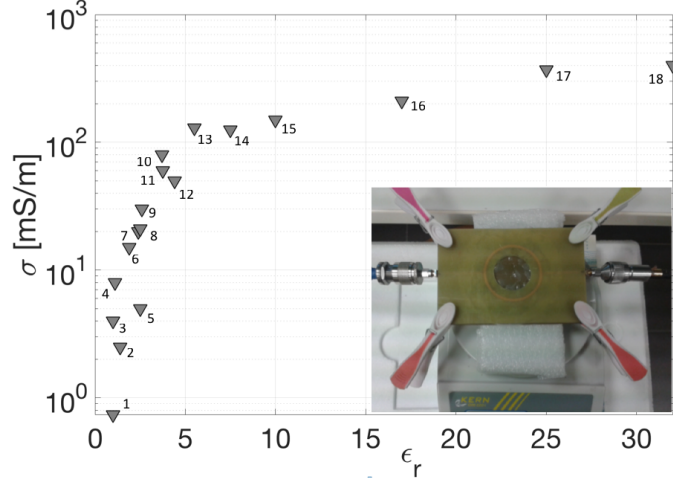

Figure 6: Dieletric properties of epidermal membranes derived through the method in [31]. Inset: Suspended ring resonator setup connected to Vector Network Analyzer (VNA). Materials: 1. Aquacel® Hydrofiber 2. Biatain® 3. Fixomull® 4. Poli(ε-caprolactone)(PCL) 5. Bio-silicone 6. PVA-coated PET 7,8. PVA/XG 4:1 hydrogel (dry) 9. PVA/XG 1:2 hydrogel (dry) 10,11,12. PVA/XG 1:1 hydrogel (dry)13. Pic MySkin® 14. PVA/XG 1:2 hydrogel (wet, 9% saline solution) 15. PVA/XG 1:2 hydrogel (wet, 12% saline solution) 16. PVA/XG 1:2 hydrogel (wet, 17% saline solution) 17. PVA/XG 1:2 hydrogel with 25% saline solution 18. PVA/XG 1:2 hydrogel with 35% saline solution

3.2   Battery-assisted (BAP) epidermal systems

Despite fully-passive systems fulfill the highest level of integration over skin resulting in extremely low-profile and nearly transparent devices, battery-assisted architectures can be considered for advanced applications as well. In particular, new-generation, sensor-oriented RFID ICs can be connected to an external battery for the two-fold purpose of *i)* increasing the sensitivity of the IC, i.e. lower power required to activate the transponder, and, accordingly, the achievable length of the wireless link and *ii)* working as an autonomous logger node able to periodically measure parameters and store the data into the IC memory even in the absence of a nearby interrogator. For instance, the download of the data can be done on-the-flight as soon as a the node enters the zone covered by a reader, e.g when crossing a gate-like setup. A local power source on the

epidermal device can be also needed to polarize some components if biasing circuits are required or to supply external (low-power) sensors. It is worth noticing that in none of the cited configurations the battery is depleted for the communication from the device to the reader - which always fully relays on modulated backscattering - implying that it can last up to few years.

Fig. 7.a shows the epidermal tag as in [22] whose layout has been slightly adapted for matching the IC (EM4325) impendence in BAP mode and connecting a standard coin cell battery (3V, 12 mm diameter, 1 mm thickness) via choke inductors (L = 120 nH). The reading range of the battery-assisted configuration is significantly increased up to 2.3 m (backward link limited), more than triple the battery-less sensor.

The second example (Fig. 7.b) is an epidermal board [32] that can be wirelessly configured for selecting both real-time (battery-less) and logging (BAP) operation. The layout etched over a 50 μm flexible Kapton substrate consists of an engineered 3 x 3 cm^2 open loop with a meander line at one ending whose length is sized to properly shape the current paths like a one-wavelength loop. The antenna is coupled with a two-way discrete (four states) tuning circuit to compensate the frequency shifts that occurs in real applications due to the intrinsic variability of the human body. Several traces and pads allow to connect a standard coin cell lithium battery and external sensors to the analog front-end of the IC (SL900A IC from AMS). The traces are replicated on both faces to achieve different sensing modalities, e.g. the simultaneous monitoring of the sweat over skin surface and of the temperature on the covering clothing. Some sensing applications of this board will be described in the next section.

Conventional power sources, such as lithium (Li), ion, and alkaline batteries connected to the above board, despite offering high energy densities, long cycle life, good shelf life, rapid charge and high energy efficiency, are often bulky and rigid. Advancements in material science and digital printing techniques are leading to achieve low-profile batteries that can be biocompatible, and eco-friendly.

The feasibility of an organic and multilayered polymer-based battery tightly integrated at physical-level with an epidermal transponder is demonstrated in [33]. The device is composed of a nested slot-line antenna embedded as the current collector at the anode of a low-profile flexible battery made of conductive Pedot:PSS doped with a variable amount of lithium ions during charging and discharging (detailed view in Fig. 7.c). The resulting system is ultrathin (approximately 200 μm), lighter than a gram, and can be used as an epidermal data-logger.
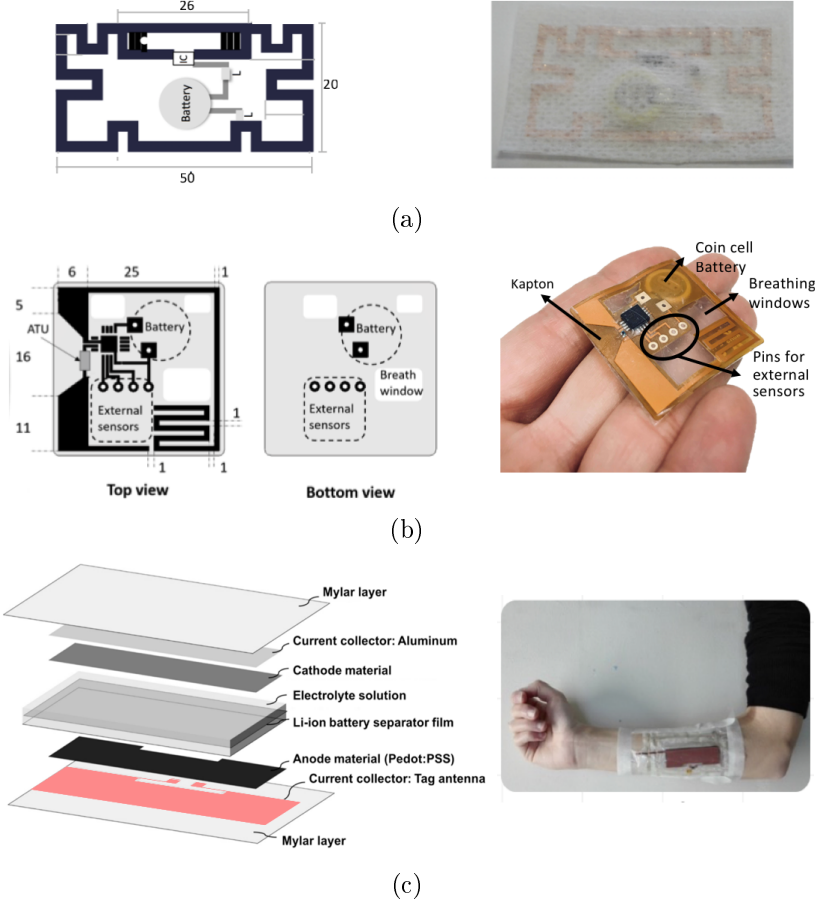
(a)

(b)

(c)

Figure 7: (a) Epidermal tag including a battery for improved reading range with the corresponding prototype encapsulated within medical plaster. (b) Top and Bottom view of the epidermal board that can be set as logger for multi-parameters monitoring. (c) An exploded view of the multilayer integrated battery-antenna system and the corresponding prototype mounted onto a volunteer's forearm. Dimensions are in mm.

4 Applications to Healthcare

Some potential applications of the described RFID-based epidermal sensors, are now discussed. The proposed examples benefit from the availability of new families of sensor-oriented RFID ICs (e.g. EM4325, SL900A, MAGNUS S3). They typically include an internal analog to digital converter (ADC), a high-speed non-volatile memory (EEPROM), an embedded temperature sensor, and a programmable digital and analog front-end to connect general-purpose micro-

controllers and sensor (thermoresitance, interdigital capacitors, strain gauge). The physical information is sampled by the specific sensor, locally digitized and stored into the microchip's memory. The sensed data are then recovered by the reader straight away in a digital form, thus dropping out the source of errors that is produced by the signal transmission over the channel.

4.1 Fever and Inflammation Monitoring

The body temperature is one of the most effective vital signals and it is normally checked in both hospital and domestic environments. In clinical practice, the temperature is periodically collected 2-3 times a day by nursing staff and manually registered on the patients' medical record. This procedure, beside increasing the nurse's workload, reduces the likelihood of collecting blood cultures during the fever spikes, that is essential for the diagnosis and antibiotic treatment of severe infections (infectious diseases, sepsis and endocarditis).

By collecting the temperature through dermal patches attached on "central" sites (forehead, armpit, abdomen, chest) and under controlled ambient conditions, it is possible to derive an approximate estimation of core temperature in non-invasive, automatic, and continuous way. With an appropriate calibration of the on-chip temperature sensor [22], the skin device can be used as a plaster-thermometer both in battery-less and battery-assisted mode (BAP) for the logging of data without any other external interrogating device. For example, Fig. 8.a shows a 24 h skin temperature pattern measured over the chest of a female patient (age 45, 1.60 m, 51 kg) hospitalized at Infection Disease ward of the Tor Vergata hospital with an abdominal abscess diagnosis. As highlighted by the shadowed band, the device enabled the early detection of the rapid temperature raise. The prediction of the fever peak was essential to promptly set-up the collection of blood specimens when there is the maximum likelihood to detect the pathogenic microorganism and accordingly provide the patient with customized antibiotics.

Beside fever estimation, an increased local skin temperature is also an indicator of a inflammatory phase of the underlying tissues which can be used as early predictor of chronicity before apparent damages of the injured tissues. In general, a persistent temperature increase of more than 1.1°C [34] at the exposed wound site can indicate infection due to the presence of bacterial organisms. An application of skin sensors to the routine of wound care is reported in Fig. 8.b. The temperature profile was measured on the internal wound bed (black line) and over the intact periwound skin area (grey line) of a obese patient having an abdominal open surgical wound treated with the vacuum-assisted closure (VAC) therapy. Thanks to the continuous and quantitative temperature measurement into the routine of wound assessment, the practitioners can evaluate the healing process without removing the bandages and timely detect suspicious infections.
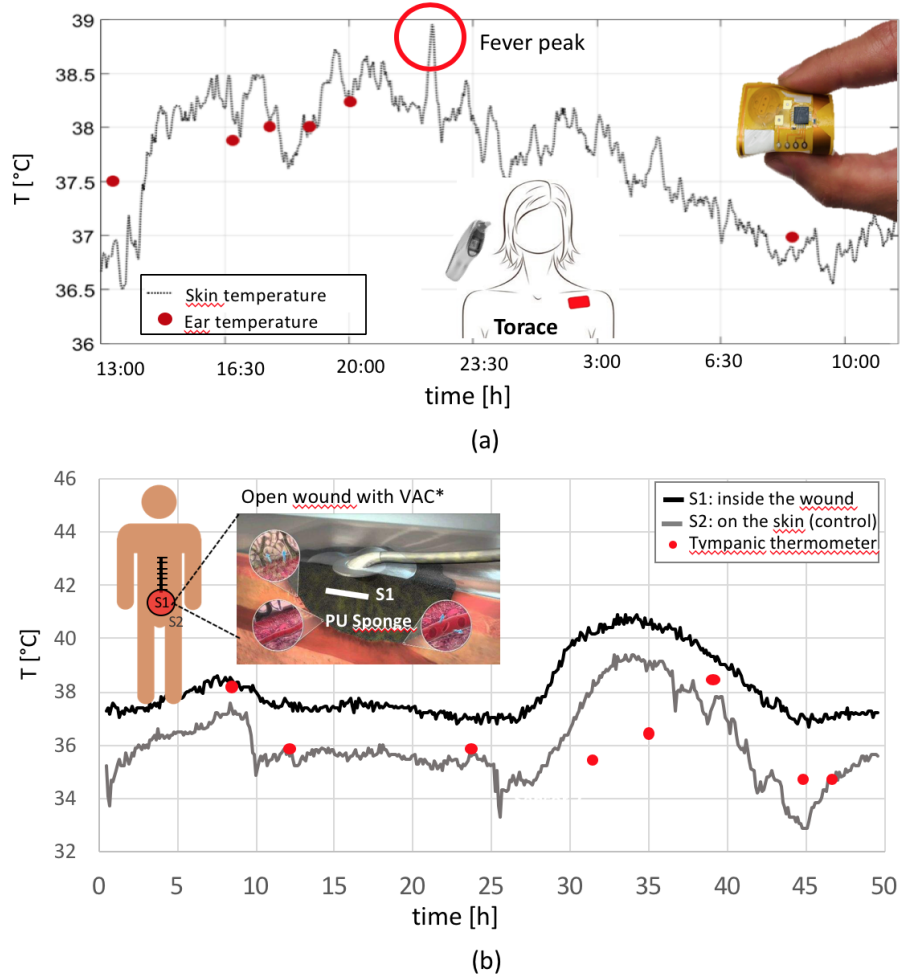
Figure 8: (a) 24 h continuous monitoring of skin by the epidermal logger in Fig. 7.b placed over the chest of a patient hospitalized at Infection Disease ward: comparison between the skin and tympanic temperatures. (b) 48 h continuous monitoring of temperature over wound bed and periwound skin area of patient treated with VAC therapy.

The above examples concern the monitoring of cutaneous temperature whose variations are mostly related to endogenous causes (fever, deep tissue inflammations). In some cases the skin can be locally heat up by means of therapeutic wraps that are designed to deliver healing warmth over the time to provide pain relief, soothe, and unlock tight muscles and sore joints (exogenous heating). Monitoring the temperature over the body surface where the band is applied could be then useful to qualify the thermal performance of device over the time (and the compliance with the package leaflet) as well assess the overall efficiency

of the therapeutic treatment. Fig. 9 shows the temperature profile measured by an epidermal logger attached on the skin at the back level beneath the single-use heating band (ThermaCare® Muscle Pain Therapy). The subject wore the device under clothing and performed its usual daily activities. Right after the application, the skin temperature starts increasing and after 1 hour it reached the therapeutic temperature (~38.5 °C), then it remains rather stable for the following 12 hours, with some fluctuations detected when the subject moved, due to the non perfect adhesion of the device to skin. Then, after 12 hours the efficiency of the thermal heating begins to decrease as indicated by the leaflet of the medical device.
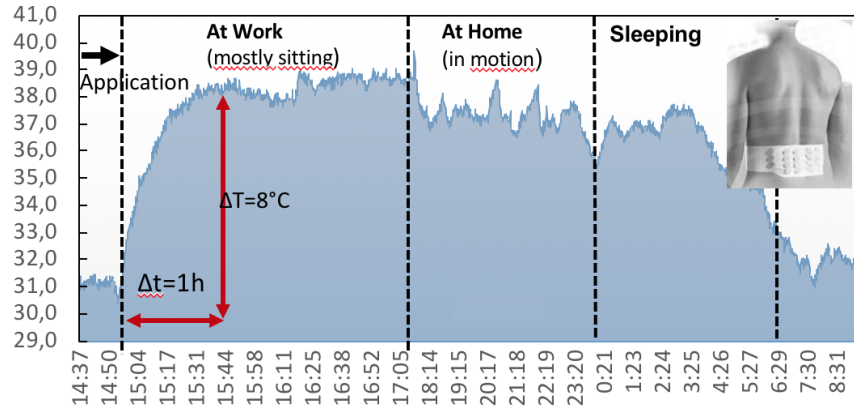

Figure 9: Collection of the thermal profile of a single-use heating band applied over the back of a male volunteer during his daily activities by an epidermal datalogger.

4.2 Breathing Pattern Monitoring

Real-time and comfortable monitoring of the human breathing could allow identifying anomalies by looking at the rhythm and the waveform of the signal to be correlated with several pathologic disorders of respiratory and cardiovascular systems (sleep apnea, asthma, Rett syndrome, chronic obstructive pulmonary disease (COPD) or cardiac arrest) as well as altered emotional states of excessive anxiety and stress. Here two different approaches are proposed for breath monitoring by using skin transponders.

The first method is based on the measurement of the temperature gradient between the inhaled ambient air and the exhaled air warmed-up by the respiratory system (at least in controlled indoor environment). As the temperature must be captured in close proximity of the upper section of the respiratory apparatus, an epidermal antenna was designed ad-hoc as a nasal strip (prototype in Fig. 10.a). The prototyped tag was connected to an RFID IC with on-chip digital temperature sensor (Magnus S3 provided by Axzon) and tested in an

experimental campaign involving twenty volunteers. The enrolled subjects were asked to mimic both normal and anomalous breathing behaviors according to a timed beeping sound programmed at a chosen frequency. As reference example, one of the traces acquired through a wireless interrogator placed at 60 cm distance from the subject is reported in Fig. 10.b. The changes of temperature within each breathing cycle are clearly detectable in term of both amplitude A and period Δt of the signal. As expected, inhalation is characterized by a rapid decrease of temperature (fresh air approaches mouth and nose), followed by an opposite phase in which air coming from inside warms up the sensor. In case of tachypnea, the amplitude A undergoes to smaller variations as the breathing acts are rapid and, accordingly, the air is maintained into the body for a shorter period. The apnea instead corresponds to a rather constant trace related to the suspension of breathing.

The physical rationale of the second approach relies, instead, on measuring the humidity change produced by the respiratory cycles through an external resistive sensor interfaced to the analog front-end of the SL900A IC by AMS. Fig. 10.b shows the prototyped board suitable for application over the cheek that is connected to a graphene-oxide (GO) sensor to be attached under the nostrils. The resistance variation of the nano-material based sensor is converted into a digital signal by the internal ADC of the IC and continuously transmitted to the external reader thorough the commands of a conventional RFID interrogation.

The sensor output (10.b) was pre-processed before extracting two significant features (dynamic range of GO resistance, R, and respiratory rate). The drift was preliminary removed by a high-pass filtering (first-order derivative), then each breathing trace was decomposed into time-frames. The dynamic range R was hence evaluated as the average difference between maximum and minimum resistances corresponding to consecutive inhalation-exhalation acts within each time frame. The Fast Fourier Transform (FFT) was finally applied to derive the respiratory rate corresponding to the peak value. Experiments involved ten healthy volunteers (3 males and 7 females, age range 25 to 33 years old) emulating a rich set of breathing patterns (including a normal breath, a deep breathing, apneas, tachypnea, and bradypnea). By processing all the breathing traces, the multi-parameter butterfly chart in Fig. 10.b was obtained. Frequencies of each respiratory pattern are rather uniform over the set of volunteers thanks to the metronome control that induces a regular inhalation/exhalation, as discussed above. Distributions of dynamic ranges of the resistances are instead much less uniform thus indicating a relevant subjectivity. The scatter plot in 10.b shows a clear tendency to separate the groups. The clustering of data was performed by applying a Decision Tree algorithm complemented by a 10-fold cross-validation. The accuracy of the classifier is about 88%.

Overall, the experiments demonstrate that both the approaches, whose main features are summarized in Fig. 11, are valid to identify the occurrence of anomalous respiratory events by using standard classification algorithms. Despite the higher complexity and the fabrication costs, the humidity-based tag is promising for the possibility of chemical functionalization of the nano-material to enrich the analysis with sensor and allow the identification of both target

20

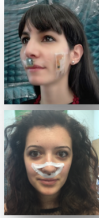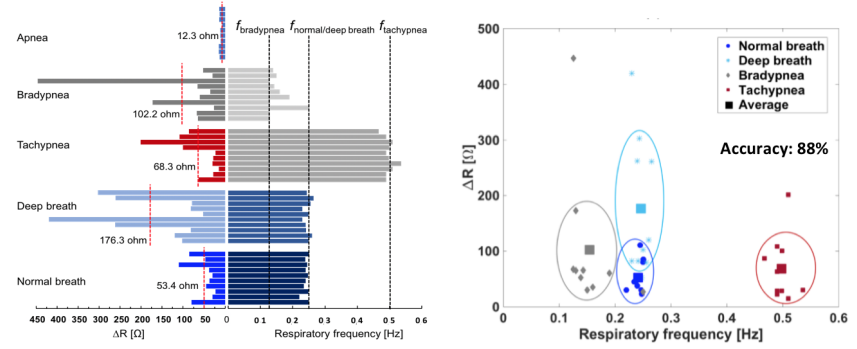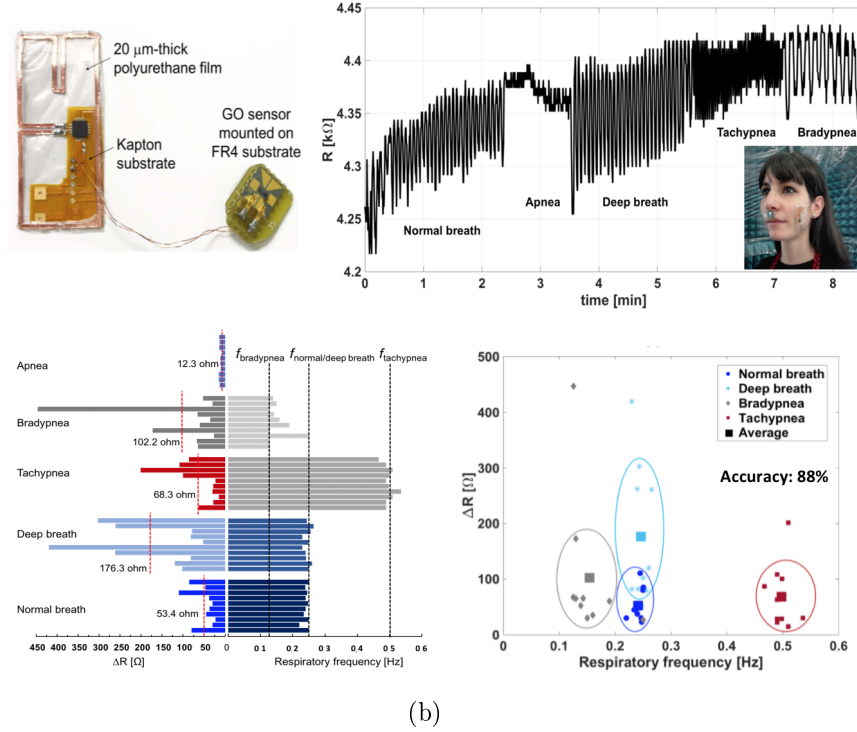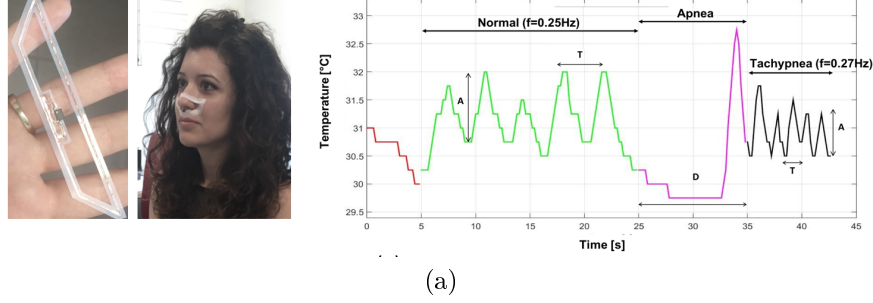biomarkers and volatile organic compounds in exhaled breath.

(a)

(b)

Figure 10: (a) Prototype of nasal strip sensor along with the measured respiratory patterns (b) Top: prototype of skin tag connecting the graphene oxide resistive sensor and resistance trace measured during different breathing cycles. Bottom: Butterfly distributions of both dynamic ranges and frequencies (dotted lines represent the average values of the bars among the ten volunteers for each breathing pattern) and Data Clusterization (apnea not reported as it lacks a peak resonance).

Type of sensor	Measured parameter	Drift	S/N	Quantization (A/resolution)	Price
Analog GO-powered resistance	Humidity	yes	50Ω/12Ω ~4	50Ω/6Ω=8	High
Digital embedded temperature	Temper.	no	2°C/0,25° =8	2°C/0.25°C=8 EM 2°C/0.1°C=20 S3	Low (<1eur)

Figure 11: Comparison of two different methods for breath monitoring based on temperature and humidity measurements by UHF skin sensors.

5 Applications to Occupational Medicine, Wellness, Sports

5.1 Monitoring workers in harsh environment (firefighters)

Monitoring the body temperature is also crucial for many categories of workers who are often exposed to ambient hazards like high thermal stress, with severe risks of physical and cognitive injuries. The epidermal board in Fig. 7.b was used for monitoring the skin temperature of a team of firefighters during the Compartment Fire Behavior Training (CFBT) program. The purpose of the tests, which is detailed in [37], is to quantity the thermal load experienced by the body during the training, to derive exposure limits, assess the effectiveness of personal protective equipment (PPE) and increase the overall awareness of firefighters for safe operation. Experiments were run inside a steel container wherein the fire is set in a controlled way by using wood-based fuel (Training plant of Italian Firefighters at Montelibretti, VT, Fig. 12.a). The involved operators wore the thermal protective clothings consisting of an inner "intervention uniform" (a shirt, a jacket, and pants) covered by a "heat protection turnout gear" (coat, hood, and over-pants), separated by an intermediated air layer which enhances the thermal insulation capacity of the PPE. The equipment also includes a helmet and a flash hood made by fire-resistant fabrics to protect head, hears, neck and part of the face. Three spots over the body were monitored by attaching tags over the internal surface of the helmet, on the chest and on the upper leg (Fig. 12.a). Due to the presence of the flash hood, the sensor on the helmet is not at direct contact with the skin. Fig. 12.b shows an example of the measured temperature profiles. The initial part of the curves relates to the preliminary activity before the direct exposure to fire. The temperature of the skin surface of both chest and leg slightly increases because

of the increased retention of body heat caused by the PPE, while the fluctuations of the helmet sensor correspond to wearing or not the helmet. During the training time with fire (the shadowed area of the plot), the temperature of the skin rises significantly but it never exceeds 43 °C, that is the critical value for tissues breakdown. Nevertheless, it is expected that the temperatures could increase above this threshold in case of longer training. It is worth noticing that the temperature continues increasing even after the operators left the container (with the helmets reaching 53 °C). The maximum temperature values on the legs are slightly lower than the ones on the chests, due to the strong vertical spatial temperature gradient of the container. By collecting data from all the subjects without any hindrance to their activity on-the-field, a comprehensive and precious insight could be derived to significantly improve the safety and the effectiveness of emergencies operations.
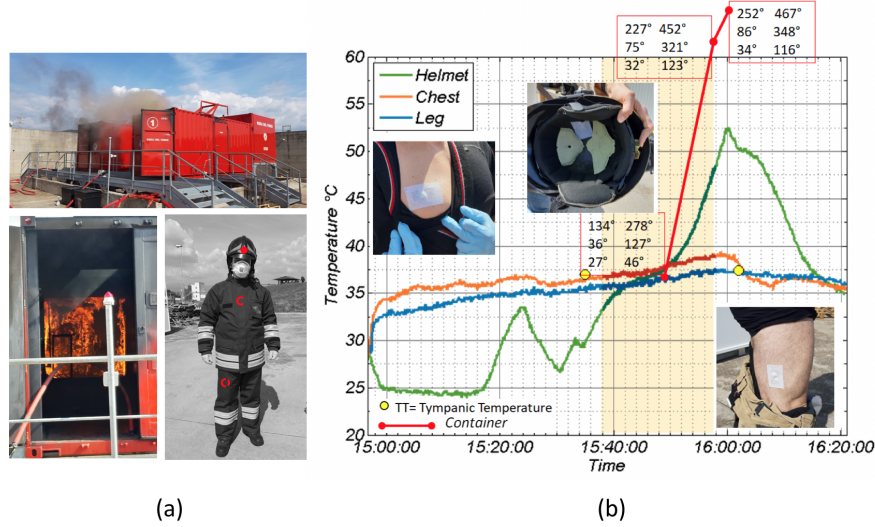

Figure 12: (a) Steel containers for CFBT at "Operational Training Center at Montelibretti" (VT, Italy) and a firefighter wearing the turnout gear (left) equipped with three data-loggers over helmet, chest and leg skin. (b) Measured temperature profiles. The shadowed area refers to the time interval inside the container. The red insert show the container temperatures measured by the six thermocouples: three near the instructor (first column) and three near the fuel (second column).

5.2   Sports

The interest for cutaneous temperature monitoring extends to sport medicine, concerning the evaluation of athletes'performance during both training and competition that could be strongly influenced by the heat exchange through the

23

skin/ambient interface by convection, radiation and evaporation. Indeed, during the exercise, the skin temperature can significantly vary according to the environmental conditions and to the intensity and duration of activity.

Fig. 13 reports an example of skin temperature monitored over the chest of a female volunteer (age 27, 1.68 m, 56 kg) during the warm-up of a beach volley workout. During the initial exercise, a fall in skin temperature is registered, due to the combined effect of the skin exposure to the fresh ambient temperature after taking off the sweatshirt and, above all, to the cutaneous vasoconstrictor response induced by the blood flow required to active muscles. Then, there is a gradual rise over time of the temperature related to dominant contribution of the thermoregulatory peripheral vasodilation which enables the progressive transfer of warmer blood from the body core to the surface.
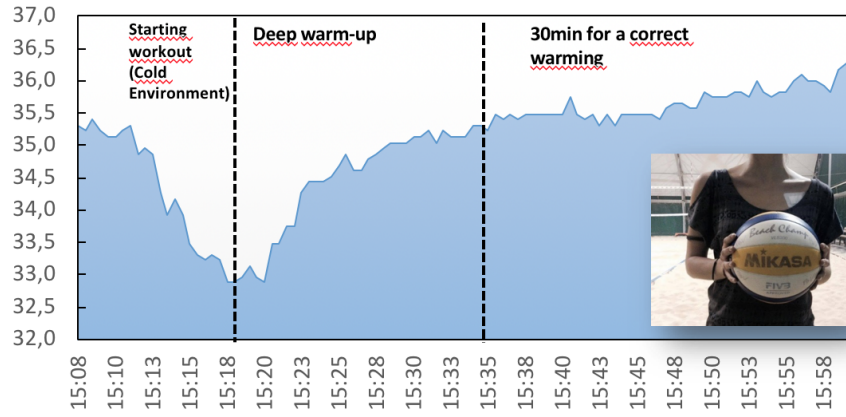

Figure 13: Temperature profile measured over skin surface at chest level during the warm up of a beach volley workout.

The monitoring of physical athlete can be further enriched by expanding the number of collected parameters. For example, Fig. 14 shows the combined profile of temperature and sweat[3] measured over the chest of a volunteer biker during 20 min exercise. For this application, two expansion terminals of the logger board were connected to an HCZ-D5 Multicomp humidity sensor, and the tag was configured to work in the BAP datalogging mode.

---

[3]The sweat is expressed as equivalent resistance R_{sweat} of the external sensor. On average, Rsweat = {0.3, 1.0, 1.3} GΩ during the precycling, cycling, and post- cycling tasks, respectively.
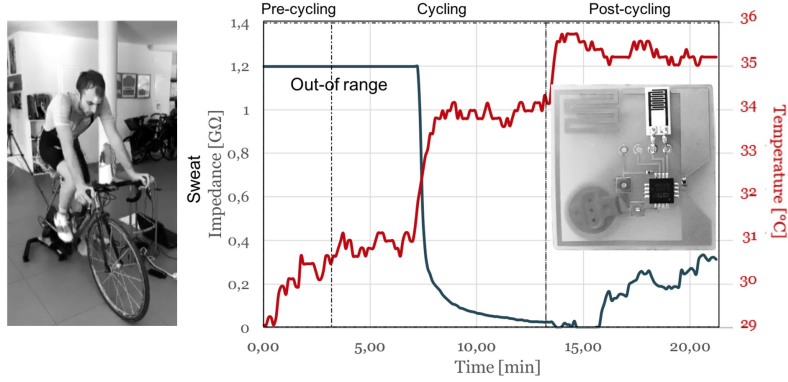
Figure 14: Examples of temperature and sweat profiles acquired by the board in data-logger mode connected to an external resistive sensors during a 20 minutes cycling activity.

The pH monitoring is another useful indicator of effectiveness of physical workout. For this purpose a multi-layer pH sensor was integrated into the skin board by screen printing over the same Kapton substrate of the antenna. The sensor consists of a modified graphite **working** electrode, a graphite one useful for the chemical **functionalization** and a silver reference electrode. Prior to use, the working electrode was electrochemically modified by means of an iridium oxide solution, to create a pH sensing film. The response of the electrodes to the pH changing is given by both the H+ activity and the iridium oxides deposited onto the working electrode surface. The pH value is measured through potentiometric method as the voltage difference among working and reference electrodes generated by the presence of the solution (sweat) covering both electrodes without any additional conditioning circuit. The average pH value of the sweat collected during outdoor activity is reported in Fig. 15 together with the corresponding temperature trend whose oscillations are due the to type of training that alternates running and resting slots.
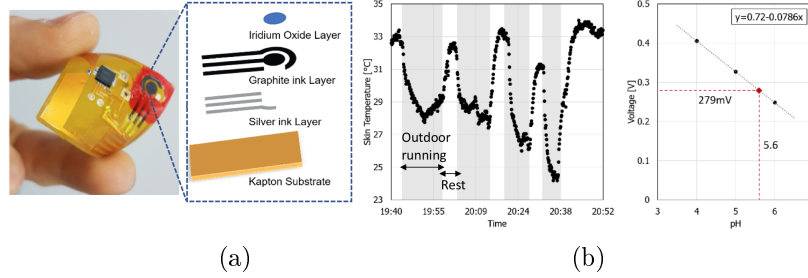
25

$$(a) \qquad\qquad (b)$$

Figure 15: a) Prototype of the UHF pH sensor integrating a screen-printed multi-layer pH chemical sensor; b) temperature data during a 30 min jogging task (grey areas) outside (average temperature 13 °C), **alternating rest periods (white areas).**

Overall, the time-evolution of skin chemical/physical parameters during exercise provides information about both the optimal muscle warming up before a competition, and an indirect estimation of the overall physical efficiency, and/or the training level of athletes.

6 Safety issue

The social and sanitary acceptance of UHF epidermal devices can not skip the concerns about the compliance of radio emission from RFID readers with human body exposure limits and safety issues [38]. The matter has been widely investigated in [15] with encouraging results. For example, Fig. 16.a shows the map of simulated 6 rms electric field for a RFID system [39] emitting 3.2 W EIRP at a duty cycle of 20% (one interrogation per second) placed at 1.5 m distance from the bed. Even the most restrictive limit of 6 V/m is fully respected in the surrounding of the bed where the patient is lying, Fig. 16.b and .c show, instead, the numerical FTDT-based simulation using realistic voxel-based and homogenous human body models exposed to the electromagnetic field emitted by a reader antennas (linear-polarized stacked planar inverted-F- SPIFA) in the near proximity (10-15 cm) of different body parts, including the head [36]. For all the considered configurations the estimated localized SAR values are quite below the limits imposed by regulations, even in the worst case of continuous-wave emission[4].

---

[4]European Recommendations impose the following rms limit to electric field emission in the UHF range $E_0 = 41$ V/m. Even more restrictive constraints may be found in some countries, as in Italy, where $E_0 = 41$ V/m. The maximum specific absorption rate $SAR = \frac{\sigma |E|^2}{2\rho}$ / (ρ, σ being the mass density and the conductivity of the tissue phantom), averaged over the body must be lower than 0.08 W/kg, while for localized exposure averaged over 10 g of tissues the limit is lower than 4 W/kg for the limbs and 2 W/Kg for head and trunk.
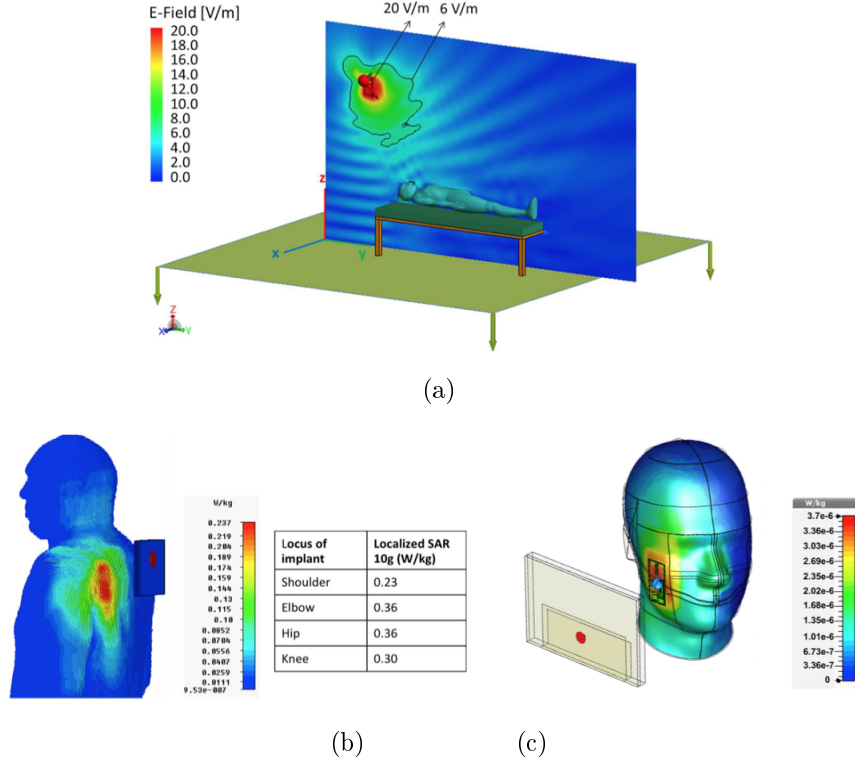
(a)

(b)   (c)

Figure 16: (a) Electric field distribution in a conventional sleeping room with a reader antenna placed 1.5 m far from the body emitting 3.2 W EIRP with a duty cycle of 20% (1 read per second); (b) SAR distribution produced in shoulder by the reader antenna placed at 10 cm distance and fed by 1 W input power along with the table of localized SAR averaged over 10 g of tissue. (c) SAR distribution produced on the face by the reader's antenna placed at 15 cm from the skin-mounted antenna and fed by 1 W input power.

7 Future Trends: Epidermal antennas for 5G systems

The upcoming fifth generation (5G) wireless communication systems is expected to significantly advance current solutions for smart living environments, smart hospitals, and wireless epidermal biosensor systems integrated within its network. 5G, in fact, pledges to provide a massive amount of raw bandwidth, a latency below 1 ms, low energy costs, and multigigabit-per-second (Gbps) data rates through both the sub-6 GHz bands (600 MHz to 6 GHz), and the mmWave frequency spectrum $(24 - 86$ GHz) [40].

During the next years, a possible convergence of epidermal biosensors within

5G would enable the deployment of massive on-skin sensors in high-speed Body Area Networks (BAN). Multi-variate data could be streamed at a high bitrate, much beyond the few hertz of sampling rate in the current UHF epidermal antennas. The envisaged advantages are even more evident when multiple sensors are deployed on a single user to collect detailed maps of biophysical processes, as well as when multitude of bodies are simultaneously involved, as in a marathon. The expected millimeter-scale of 5G epidermal devices will moreover enable the concept of skin-arrays to shape the radiation beam. The low latency could make the skin sensors acting as precise markers during telesurgery to improve the virtualization of the scene and the fidelity of the remote interactions. Finally, thanks to the interoperability of 5G systems, the wireless data exchange will be seamlessly achieved by both 5G personal devices, in user-oriented applications, as well as by fixed interrogators in infrastructure-oriented frameworks. Thus, an electronic plaster would be able to communicate both with other skin sensors of the network, and with implanted devices (like a skin gateway for on/off/in body link), and with the nearby smartphone, smartwatch or smart earbuds as well as with external base stations.

However, the feasibility of a battery-less backscattering-based link at 5G frequency bands (5G-RFID) is still in question due to both the higher human body losses at these frequencies as well to the increased free space path loss.

Starting from the theoretical findings in [20], the preliminary study in [41] expanded the analysis to the frequency bands relevant for 5G communications, at the purpose to derive the achievable upper-bound performances of 5G-RFID epidermal transponders when either single- or multi- antenna radiators are used and compared them with conventional UHF counterparts. Fig. **18** summarizes the main results of numerical simulations that assumed, as reference, a typical UHF antenna footprint of 30 x 30 mm^2, a sensor sensitivity of -15 dBm, and a transmitting EIRP of 4 W (as allowed by the FCC regulations). The assumed footprint is suitable to allocate a single optimal antenna loop at 3.6 GHz; up to a 5 x 5 array at 28 GHz; and a 12 x 12 array at 60 GHz. A single 3.6 GHz antenna returns a similar read distance than in UHF but with a reduced size (17.5 mm vs. 30 mm). mmWave links are also meaningful with a minuscule standalone element providing a read distance of about 20 cm. Even though much smaller than the UHF counterpart, this configuration could be attractive for ultra-short-range high-speed data links by a 5G smartphone, as a modern version of NFC communication. Array configurations with 25 elements (@ 28 GHz) and 6 x 7 elements (@ 60 GHz) would guarantee 1 m read distance as the state-of-the-art UHF epidermal sensors. Finally, the 144 loops (12 x 12) at 60 GHz, that can be packed within the footprint of a single UHF loop, show a further improvement of the activation distance.
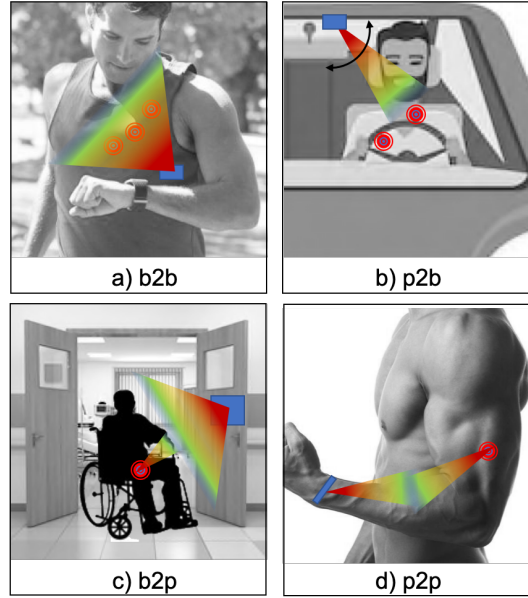
Figure 17: Concepts of epidermal sensor networks at 5G frequencies: a) smart-watch (or smartphone) simultaneously and quickly retrieving multiple biophysical data for personal tracking in sport and wellness; b) smart car taking care of the stress level of a driver to prevent accidents; c) smart house periodically monitoring on-the-fly the healthy status of elderly people to identify early signs of health crisis and prompt for assistance; d) high-accuracy real-time tracking of muscle contraction for precise sport training and rehabilitation support.
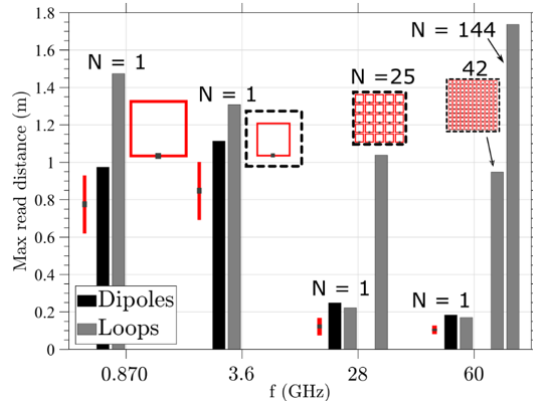

Figure 18: Comparing forward link ranges of several backscattering links for tag sensitivities of -15 dBm. EIRP fixed to 4 W (36 dBm). Dipoles, loops and loop arrays are compared with a 3 x 3 cm^2 footprint.

8   Conclusions

The fertile research on Skin Electronics has paved the way to a novel approach for the continuous assessment of people's health and well-being by pushing the technologies from clothes and personal accessories directly to the human skin.

Despite early research mostly focused on the high-tech fabrication of engineered thin films with sensor capabilities, there is nowadays an increasing attention to the powering and communication issues related to the epidermal devices, which are the current bottlenecks for the real spreading of skin-worn devices. The close proximity to the lossy human body, separated at most by sub-millimetric substrates, enforces an upper-bound gain for epidermal radiators that is independent on the antenna shape and can not be improved by making the antenna larger. The epidermal antenna can be conveniently manufactured by biocompatible and organic inks as well as by thin conducting wires deposited over flexible membranes.

Overall the real-word adoption of this technology is not far. By exploiting sensing-oriented RFID ICs, it is possible to remotely monitor the human health and activity (e.g. body temperature and breathing), replace physical sensing deficits by transducing the parameters measured by the epidermal sensors into haptic feedbacks and even augment the natural sensorial capabilities (ultrability) [42]. The reading distances currently achievable with state-of-art components reach 1.5 m. Major sensitivity on both RFID ICs and readers will be needed to further increase the communication link.
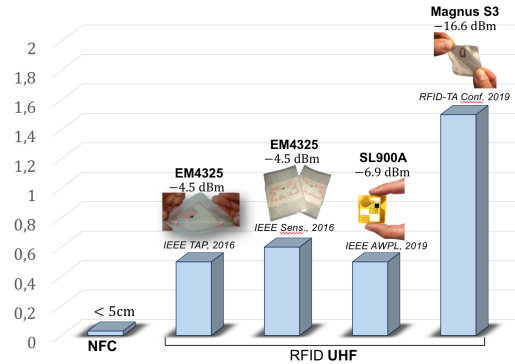

Figure 19: Typical reading distance of battery-less RFID epidermal sensors.

Open challenges concern the calibration of the skin devices and the processing needed to retrieve meaningful data that are robust against the interpersonal variability and measurements conditions (model-based measurements).

Finally, new interesting opportunities are expected from the emerging 5G technology, thanks to its wide band and its spreading architecture.

References

[1] Kim, Dae-Hyeong, *et al.* , "Epidermal electronics," *Science*, vol. 333, no. 6044, pp. 838–843, 2011.

[2] J.A. Rogers, R.Ghaffari, and D.H.Kim, *Stretchable Bio-electronics for Medical Devices and Systems*, Springer, 2016.

[3] T. Vuorinen, J. Niittynen, T. Kankkunen, T. M. Kraft, M. Mäntysalo, " Inkjet-Printed Graphene/PEDOT:PSS Temperature Sensors on a Skin-Conformable Polyurethane Substrate", *Scientific Reports*, Oct. 2016.

[4] S. R. Krishnan, C. J. Su, Z. Xie, et al., "Wireless, Battery-Free Epidermal Electronics for Continuous, Quantitative, Multimodal Thermal Characterization of Skin", *Small Journal*, vol. 14, n. 47, 2018.

[5] W. Gao, S. Emaminejad, H. Y. Y. Nyein, et al., "Fully Integrated Wearable Sensor Arrays for Multiplexed in Situ Perspiration Analysis", *Nature*, vol. 529, pp. 509−514, 2016.

[6] J. J. Norton, D. S. Lee; J. W. Lee, et al., "Soft, Curved Electrode Systems Capable of Integration on the Auricle as a Persistent Brain−Computer Interface", *Proceedings of the National Academy of Sciences*, vol. 112, n. 3, pp. 3920−3925, 2015.

[7] H. Sillanpää, A. Vehkaoja, D. Vorobiev, et al., " Integration of inkjet and RF SoC technologies to fabricate wireless physiological monitoring system", *Proceedings of the 5th Electronics System-integration Technology Conference (ESTC)*, Helsinki, Finland, 16-18 Sept. 2014.

[8] T. Yokota, P. Zalar, M. Kaltenbrunner, et al., "Ultraflexible Organic Photonic Skin", *Science Advances*, vol. 2, n. 4, 2016.

[9] S. Yoon, J. K. Sim, Y. Cho, "A Flexible and Wearable Human Stress Monitoring Patch", *Scientific Reports*, March 2016.

[10] Dobkin, Daniel M. *The RF in RFID: UHF RFID in Practice.* Newnes, 2012.

[11] X. Huang, Y. Liu, H. Cheng, W.-J. Shin, J. A. Fan, Z. Liu, C.-J. Lu, G.-W. Kong, K. Chen, D. Patnaik et al., "Materials and designs for wireless epidermal sensors of hydration and strain," *Advanced Functional Materials*, vol. 24, no. 25, pp. 3846–3854, 2014.

[12] D. P. Rose, M. E. Ratterman, D. K. Griffin, L. Hou, N. Kelley-Loughnane, R. R. Naik, J. A. Hagen, I. Papautsky, and J. C. Heikenfeld, "Adhesive rfid sensor patch for monitor- ing of sweat

electrolytes," *IEEE Transactions on Biomedical Engineering*, vol. 62, no. 6, pp. 1457–1465, June 2015.

[13] S. B. Kim *et al* Soft, Skin-Interfaced Microfluidic Systems with Wireless, Battery-Free Electronics for Digital, Real-Time Tracking of Sweat Loss and Electrolyte Composition" *Small*, vol. 14, no.45 , 2018.

[14] S.R. Krishnan, *et al*, "Wireless, Battery-Free Epidermal Electronics for Continuous, Quantitative, Multimodal Thermal Characterization of Skin," *Small*, vol. 14, no.47 , 2018.

[15] S. Amendola, R. Lodato, S. Manzari, C. Occhiuzzi, G. Marrocco, "RFID Technology for IoT-Based Personal Health- care in Smart Spaces," *Internet of Things Journal, IEEE* , vol.1, no.2, pp.144-152, 2014.

[16] Online] Available: BlueSparkTechnologies, http://www. bluespark-technologies.com/

[17] [Online] Available: Flexible Lithium-ion Battery by Panasonic, http://news.panasonic.com/global/press/data/2016/09/en160929-8/en160929-8.html

[18] S. Manzari, C. Occhiuzzi, and G. Marrocco, "Feasibility of body-centric systems using passive textile rfid tags," *Antennas and Propagation Magazine, IEEE*, vol. 54, no. 4, pp. 49– 62, Aug 2012.

[19] T. Kellomaki, "On-body performance of a wearable single-layer rfid tag" *IEEE Antennas and Wireless Propagation Letters*, no. 11, pp. 73–76, 2012.

[20] S. Amendola and G. Marrocco, "Optimal Performance of Epidermal Antennas for UHF Radiofrequency Identification and Sensing", in *IEEE Transactions on Antennas and Propagation*, vol.65, no. 2, pp. 473-481, 2016.

[21] S. Amendola, S. Milici and G. Marrocco, "Performance of Epidermal RFID Dual-loop Tag and On-Skin Retuning," in *IEEE Transactions on Antennas and Propagation*, vol. 63, no. 8, pp. 3672-3680, Aug. 2015.

[22] S. Amendola, G. Bovesecchi, A. Palombi, P. Coppa, G. Marrocco, "Design, Calibration and Experimentation of an Epidermal RFID sensor for remote Temperature Monitoring", in *IEEE Sensors Journal*, vol. 16, no. 19, pp. 7250-7257, July 2016.

[23] F. Amato, C. Miozzi, S. Nappi and G. Marrocco, "Self-Tuning UHF Epidermal Antennas", *RFID TA Conference, 2019,* Pisa (IT), September, 2019

[24] S. Amendola, V. Greco, G. M. Bianco and G. Marrocco, "Application of Radio-Finger Augmented Devices to Cognitive Neural remapping", *RFID TA Conference, 2019,* Pisa (IT), September, 2019.

[25] S. Amendola, V. Di Cecco, and G. Marrocco, "Numerical and Experimental Characterization of Wrist-Fingers Communication Link for RFID-based Finger Augmented Devices", *IEEE Transactions on Antennas and Propagation*, February 2019.

[26] S. Amendola, A. Palombi, L. Rousseau, G. Lissorgues, G. Marrocco, "Manufacturing Technologies for UHF RFID Epidermal Antennas", European Microwave Conference (EuMC), 2016 European, London, October 2016.

[27] NBSIJ Diamond Jet Silver Nanoparticle Ink, Mitsubishi Imaging (MPM), Inc

[28] S. Amendola, A. Palombi, G.Marrocco, "Inkjet Printing of Epidermal RFID Antennas by Self-Sintering Conductive Ink", in *IEEE Transactions on Microwave Theory and Techniques*, vol.66, N.3, pp.1561-1569, Mar. 2018.

[29] S. Milici, S. Amendola, A. Bianco and G. Marrocco, "Epidermal RFID Passive Sensor for Body Temperature Measurements", *IEEE RFID Technology and Applications Conference* (RFID-TA), 2014.

[30] A. Ajovalasit, M. C. Caccami, S. Amendola, M. A. Sabatino, G. Alotta, M. Zingales, D. Giacomazza, C. Occhiuzi, G. Marrocco, C. Dispenza, "Development and characterization of xyloglucan-poly(vinyl alcohol) hydrogel membrane for Wireless Smart wound dressings", *European Polymer Journal*, Elsevier, vol. 106, pp. 214-222, 2018.

[31] S. Amendola, *et al.* "Dielectric characterization of biocompatible hydrogels for application to epidermal RFID devices.", *European Microwave Conference (EuMC). IEEE*, 2015.

[32] C. Miozzi, S. Nappi, S. Amendola, C. Occhiuzzi, and G. Marrocco, "A General-purpose Configurable RFID Epidermal Board with a Two-way Discrete Impedance Tuning", *IEEE Antennas and Wireless Propagation Letters*, February 2019.

[33] M. C. Caccami, M. P. Hogan, M. Alfredsson, G. Marrocco and J. C. Batchelor, "A Tightly Integrated Multilayer Battery Antenna for RFID Epidermal Applications", *Transactions on Antennas and Propagation*, November 2017.

[34] M. Fierheller, and R. Gary Sibbald. "A clinical investigation into the relationship between increased periwound skin temperature and local wound infection in patients with chronic leg ulcers", *Advances in skin & wound care,* vol. 23, no. 8, pp. 369-379, 2010.

[35] C. Occhiuzzi, C. Caccami, S Amendola, G Marrocco, "Breath-monitoring by means of Epidermal Temperature RFID Sensors", *3rd International Conference on Smart and Sustainable Technologies,* Split, 2018.

[36] C. Caccami, M. Y. S. Mulla, C. Occhiuzzi, C. Di Natale and G. Marrocco, "Design and Experimentation of a Battery less On-Skin RFID Graphene-Oxide sensor for the Monitoring and Discrimination of Breath Anomalies," *IEEE Sensors Journal,* vol. 18, no. 21, pp. 8893-8901, 1 Nov.1, 2018.

[37] F. Camera, C. Occhiuzzi, C. Miozzi, S. Nappi, A. Bozzo, P. Tomola, A. Bin and G. Marrocco, "Monitoring of temperature stress during firefighters training by means of RFID epidermal sensors", RFID-TA 2019, Pisa (IT), September 2019.

[38] Limitation of Human Exposure to Electromagnetic Fields from Devices Operating in the Frequency Range 0 Hz to 10 GHz, Used in Electronic Article Surveillance (EAS), Radio Frequency Identification (RFID) and Similar Applications, Standard CENELEC EN 50364

[39] C. Occhiuzzi, C. Vallese, S. Amendola, S. Manzari, G. Marrocco, "NIGHT-care: a passive RFID system for remote monitoring and control of overnight living environment", *Procedia Computer Science,* vol.32, pp.190-197, 2014.

[40] J. G. Andrews, S. Buzzi, W. Choi, S. V. Hanly, A. Lozano, A. C. K. Soong, and J. C. Zhang, "What will 5g be?" *IEEE Journal on Selected Areas in Communications,* vol. 32, no. 6, pp. 1065–1082, June 2014.

[41] F. Amato, S. Amendola and G. Marrocco, "Upper-bound Performances of RFID Epidermal Sensor Networks at 5G Frequencies,""*2019 IEEE 16th International Conference on Wearable and Implantable Body Sensor Networks (BSN),* Chicago, IL, USA, 2019, pp. 1-4.

[42] G. M Bianco and G. Marrocco, "Fingertip Self-tuning RFID Antennas for the Discrimination of Dielectric Objects", *EUCAP* 2019, Kracov, Polland